

Investigation of the electronic structure in $\text{La}_{1-x}\text{Ca}_x\text{CoO}_3$ ($x = 0, 0.5$) using full potential calculations

M Sahnoun^{1,3}, C Daul¹, O Haas² and A Wokaun²

¹ Chemistry Department, University of Fribourg, Perolles, CH-1700 Fribourg, Switzerland

² Department General Energy, Paul Scherrer Institut, CH-5232 Villigen, Switzerland

E-mail: mohammed.sahnoun@unifr.ch

Abstract

The electronic and magnetic properties of both LaCoO_3 and $\text{La}_{0.5}\text{Ca}_{0.5}\text{CoO}_3$ have been investigated by means of *ab initio* full-potential augmented plane wave plus local orbitals (APW + lo) calculations carried out with the Wien2k code. The functional used is the local-density approximation LDA+ U . Doping with Ca^{2+} introduces holes into the Co–O network. We analyse the densities of states and we confirm that the intermediate state (IS) is stabilized by the Ca^{2+} substitution. This intermediate state in our results turns out to be metallic, and has a large density of states at the Fermi energy. The calculated magnetic moment in $\text{La}_{0.5}\text{Ca}_{0.5}\text{CoO}_3$ is found to be in good agreement with experiment.

(Some figures in this article are in colour only in the electronic version)

1. Introduction

LaCoO_3 has been extensively studied in connection with the spin-state transition [1–11]. Spin-polarized calculation on the hypothetical cubic perovskite phase of LaCoO_3 showed that the ferromagnetic phase is lower in energy than the corresponding nonmagnetic phase [41]. We take the model with the highest symmetry and the smallest unit cell. The magnetic and the electric properties of $\text{La}_{1-x}\text{Ca}_x\text{CoO}_3$ system have also been reported [13–24], and it has been confirmed that the intermediate state (IS) is stabilized by the Ca^{2+} substitution, and the magneto-transport properties can be interpreted as a ferromagnetic metals of itinerant electrons with strong electron–electron correlations. Muta *et al* [16] have also argued that the observed ferromagnetic saturation moment of $1.2 \mu_B$ in metallic $\text{La}_{1-x}\text{Ca}_x\text{CoO}_3$ ($x = 0.2–0.5$) is due to stabilization of the IS state. However, the reported data alone are not sufficient to explain the quantitative effects of the Ca substitution on LaCoO_3 . Therefore, a careful comparison of

³ Author to whom any correspondence should be addressed.

the magnetic and electronic properties of LaCoO_3 and $\text{La}_{0.5}\text{Ca}_{0.5}\text{CoO}_3$ will be useful to assess the role of the hole-doping in stabilizing the intermediate spin (IS).

To evaluate the physical properties of both LaCoO_3 and $\text{La}_{0.5}\text{Ca}_{0.5}\text{CoO}_3$ compounds, a theoretical study of the electronic structure and of the magnetic properties is presented using the full potential linearized augmented plane wave (FP-LAPW) method. In this approach, the LDA + U approximation is used for the exchange–correlation energy.

This choice of stoichiometry results in several potential advantages. A doping level of $x = 0.5$ eliminates any possible effects of chemical inhomogeneity, since the cations are ordered [25] for $x = 0.5$; this is not the case for $x < 0.5$ [26–28]. Ca is chosen as the dopant since La^{3+} and Ca^{2+} have virtually identical ionic radii (1.36, 1.34 Å, respectively [29]), thus eliminating any possible effect of localized lattice distortions. Ravindran *et al* [30] have found that the energy barriers between LS and HS as well as between IS and HS are very large in LaCoO_3 , and have concluded from supercell calculations on hole doped $\text{La}_{1-x}\text{Sr}_x\text{CoO}_3$ that the Co ions have almost the same spin polarization. Hence theory rules out the possibility of stabilizing a mixed-spin state such as LS and HS, IS and HS or the combination of these by temperature/hole doping.

We have found that the nonmagnetic insulating behaviour of LaCoO_3 is in agreement with experiment and also with previous calculations. In the case of $\text{La}_{0.5}\text{Ca}_{0.5}\text{CoO}_3$, we obtain an intermediate-spin state which turns out to be metallic as well. We hope that this information will eventually lead to a better understanding of LaCoO_3 and of similar materials.

2. Details of the calculation method

The unit cell of LaCoO_3 is a slightly distorted perovskite that could be indexed with rhombohedral ($R\bar{3}c$) structure, consisting of two formula units (f.u.) each containing one La, one Co and three O atoms. The structure is almost cubic, thus we adopt the model with the highest symmetry and the smallest unit cell which is the cubic structure ($Pm\bar{3}m$). The cell geometry optimization is used to obtain the optimal lattice constants for both systems considered in this paper. In table 1, we present our results for the equilibrium lattice constants. Calculations were carried out with the full potential linearized augmented plane wave (FP-LAPW) method implemented in the Wien2k code [31]. In the LAPW method [32–34] the unit cell is divided into two types of regions, the atomic spheres centred upon nuclear sites and the interstitial region between the nonoverlapping spheres. Inside the atomic spheres, the wavefunctions are replaced by atomic-like functions, while in the inter-sphere region the wavefunction of a Bloch state is expanded in plane waves. The charge density and the potentials are expanded into lattice harmonics up to $l = 6$ inside the spheres and into a Fourier series in the interstitial region. We have included the local orbitals [34, 35] for La 5s, 5p, Ca 3s, 3p, Co 3p and O 2s. The convergence of the basis set is controlled by a cut-off parameter $R_{\text{mt}} \cdot k_{\text{max}} = 7$ where R_{mt} is the smallest atomic sphere radius in the unit cell and k_{max} is the magnitude of the largest \mathbf{k} vector. To ensure convergence for the Brillouin zone integration 84 \mathbf{k} -points in the irreducible wedge of the first Brillouin zone (IBZ) were used for the cubic structure (even half the number of these \mathbf{k} -points gave the correct result qualitatively). A similar density of \mathbf{k} -points is used in the supercell calculations. The integrals over the Brillouin zone are performed using the Monkhorst–Pack special \mathbf{k} -points approach [36]. Self-consistency is achieved by demanding the convergence of the total energy to be smaller than 10^{-5} Ryd/cell. This corresponds to a convergence of the charge to be lower than 10^{-4} electrons/atom. For all calculations the sphere radii used are 2.73, 2.73, 1.80 and 1.60 Bohr for La, Ca, Co and O, respectively. For the exchange–correlation potential the standard L(S)DA (local (spin) density approximation [37]) or the GGA (generalized gradient approximation [38]) based

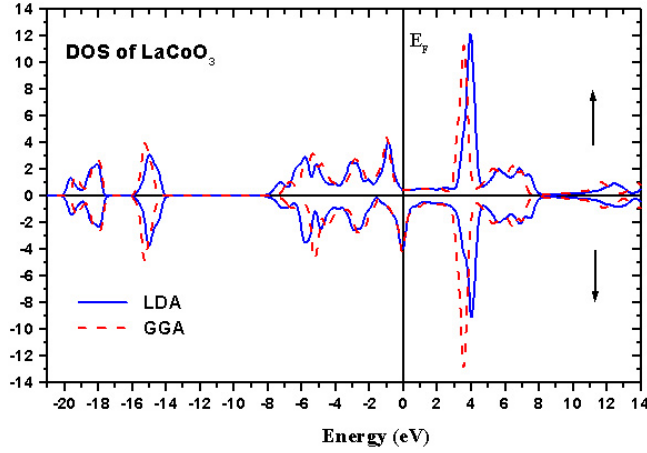


Figure 1. The total (in states/eV cell) densities of states obtained in both LDA (solid line) and GGA (dashed line) calculations for LaCoO_3 .

methods cannot describe the magnetic state for LaCoO_3 without taking into account Coulomb interaction between 3d electrons as demonstrated in [7]. However, analysis of the LSDA (GGA) results (figure 1) is instructive for understanding of the basic electronic structure of lanthanide cobaltite perovskites, but these methods produce an unphysical metallic character due to the fact that crystal field and electronic structure effects are not sufficient in this case to open a gap. To improve the description of Co 3d electrons, we thus use the LDA + U method as described by Anisimov *et al* [39]. Although LSDA (GGA) calculations are generally *ab initio*, LDA + U calculations are not fully *ab initio* since values of the Hubbard parameter U and the exchange parameter J must be inserted. These can either be taken from experimental or estimated values using the restricted LSDA (GGA) supercell calculation. As shown recently [40] the exact value of U depends on the computational method and the approximations made when estimating U . However, it is generally agreed that for this type of compound the value of U is in the range of several eV up to about 8 eV. In the present study we assumed U to be 6 eV, in which the total moment (M) is zero and stabilizing a nonmagnetic phase of LaCoO_3 (figure 2), but checked how the results depend on U and found that for $U \leq 2.5$ eV we basically recover the LSDA (GGA) solution. For larger values of U ($U \geq 6.5$ eV), the ferromagnetic solution remains stable. This choice of $U = 6$ eV also gives reasonable magnetic moment for $\text{La}_{0.5}\text{Ca}_{0.5}\text{CoO}_3$. We want to stress that all our conclusions in this argument do not depend on U as long as it is chosen in a reasonable range. The value of J is fixed to 0.5 eV. The main effect of LDA + U potential correction is the energy splitting between occupied and empty states in such a way that the former are pushed down and the later pushed up comparing with LSDA (GGA).

3. Results and discussions

In table 1, we present our results of the equilibrium lattice constants for LaCoO_3 and $\text{La}_{0.5}\text{Ca}_{0.5}\text{CoO}_3$. As is well known, LSDA generally underestimates, but GGA overestimates, the equilibrium lattice parameter. We have also found that in both cases the band structure remains the same near the Fermi energy (figure 1).

The Co 3d states are very important and deserve to be discussed in more detail because they determine the magnetic properties. We use the concept of t_{2g} and e_g orbitals, as referred

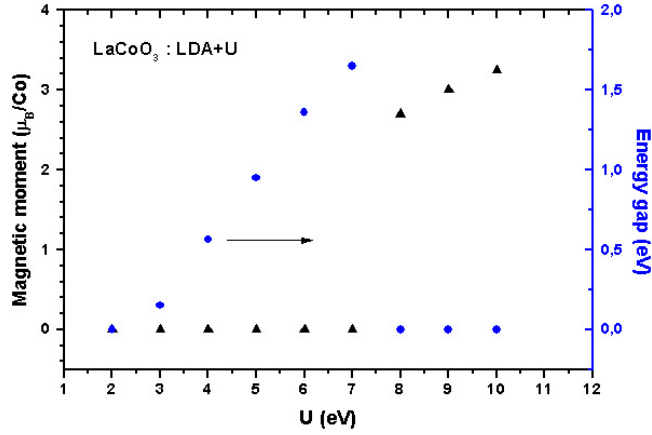


Figure 2. Energy gap and local magnetic Co moment versus U value using the LDA + U approximation in LaCoO_3 .

Table 1. Lattice parameter, energy gap, character of the energy spectrum, occupancies of various d orbitals of Co, and magnetic moments for Co. All calculations shown are performed within the LSDA or LDA + U .

Compound	a_0 (Å)	Energy gap (eV)	d occupancies			$\mu_{d-\text{Co}}$ (μ_B)	
			e_g	t_{2g}	Total		
LaCoO_3 $t_{2g}^6 e_g^0$ (low spin)	7.082 (LDA)	1.06	\uparrow, \downarrow	1.05 5.41	6.46	0	
$\text{La}_{0.5}\text{Ca}_{0.5}\text{CoO}_3$ $t_{2g}^5 \sigma^*$ (intermediate spin)	6.696 (LDA)	0	\uparrow \downarrow	1.03 0.49	2.66 1.97	6.15	1.2

to in the cubic setting in the following discussion. In an octahedral crystal field the d electrons will be split into doubly degenerate e_g and triply degenerate t_{2g} levels. The t_{2g} and e_g projected density of states of Co in the cubic phases of LaCoO_3 and $\text{La}_{0.5}\text{Ca}_{0.5}\text{CoO}_3$ are represented in figures 3 and 4 respectively.

Considering the density of states (DOS) for LaCoO_3 , as shown in figure 3, it is distributed in the energy range from -21 to 14 eV. The top panel represents the total density of states. The partial densities of states for Co and O atoms are shown in associated panels. The Fermi energy is set to zero. There are two main peaks below the Fermi energy, they originate mostly from the occupied t_{2g} band and from the O p orbitals, the e_g band is nearly unoccupied just above the Fermi energy. The O p and Co d states are mixed with each other in the valence band. By contrast, the La spectral weight contributes mainly to the unoccupied electronic states in the conduction band. This suggests that La has more ionic character and is stabilized by the Madelung potential, whereas the covalent contribution to the bonding is more prominent within the Co–O octahedra. The sharp feature at 5 eV above the Fermi level corresponds to the La 4f band and the DOS segment at 4–8 eV is composed mainly of La 5d states. This is in agreement with the configuration of the low-spin state and with photoemission experiments [24]. The large peak below the Fermi level corresponds to the Co t_{2g} bands. These relatively nonbonding states produce weak Co–O–Co interactions which give rise to a narrow band. By contrast, the Co e_g states produce very strong Co–O–Co interactions which give rise to a much larger dispersion, and result in the broader e_g band. The simple ligand field model predicts that

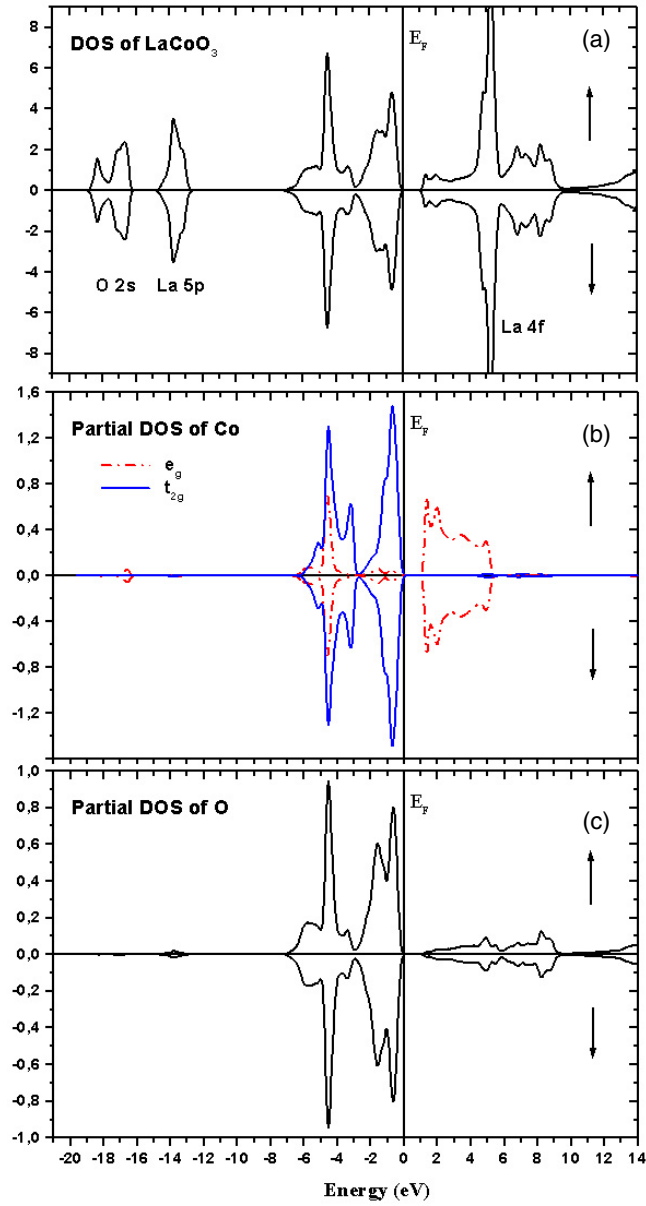


Figure 3. The total (in states/eV cell) and partial (in states/eV atom) densities of states obtained in LDA + U calculations for LaCoO_3 with Co ions in the low-spin state. For the Co d partial density of states, the solid (blue) line denotes t_{2g} orbitals, and the dot-dashed line (red) e_g orbitals. The Fermi level is denoted by the vertical solid line.

for the LS state of LaCoO_3 the t_{2g} levels are completely filled and the e_g states completely empty. In our calculation, however, the e_g states are distributed over the entire valence and conduction bands, and these e_g orbitals partly fall below the Fermi level and are mixed with the t_{2g} orbitals. The lobes of the t_{2g} orbitals point between the oxygen ligands, whereas the e_g orbitals point directly toward the ligands. Hence, the overlap with O 2p orbitals will be greater

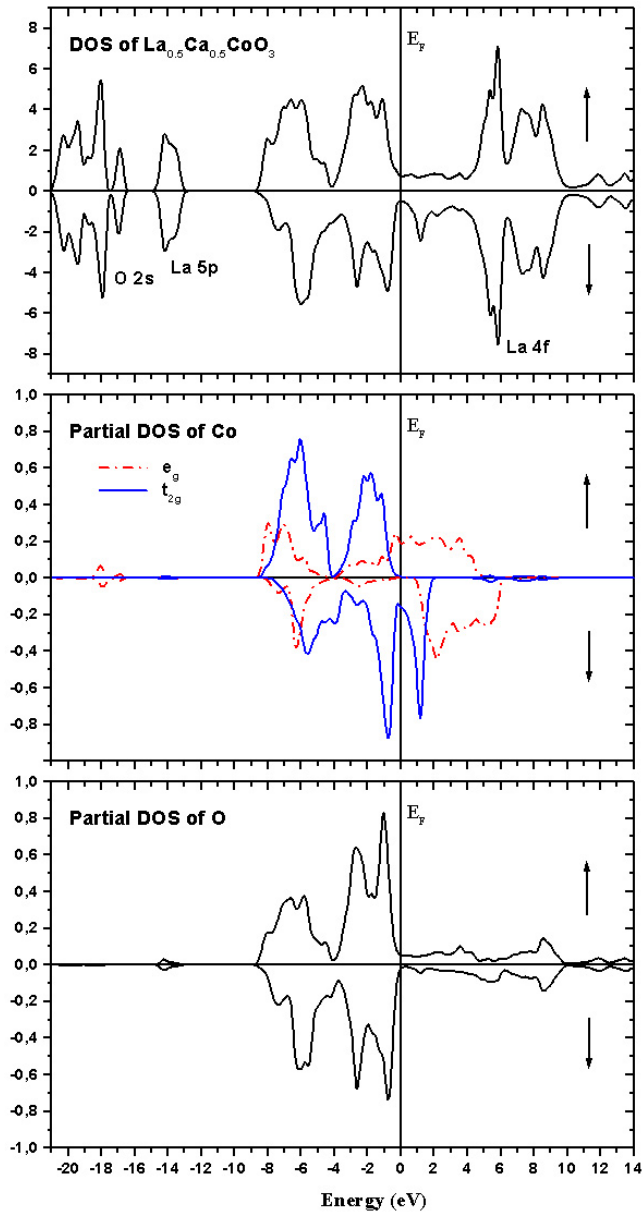


Figure 4. The total (in states/eV spin cell) and partial (in states/eV spin atom) densities of states obtained in LDA + U calculations for $\text{La}_{0.5}\text{Ca}_{0.5}\text{CoO}_3$. Arrows corresponds to spin-up and spin-down spin projections. The other notations are the same as in figure 3.

for the e_g states, and the increased overlap results in local repulsion between overlapping charge densities. This repulsive interaction pushes the e_g orbitals to higher energy. However, some of the repulsion is compensated by hybridization in the resulting bonding states, which in turn leads to a considerable amount of e_g state in the conduction band. The calculations show that E_F lies in the vicinity of the sharp nonbonding t_{2g} peak for the Co 3d electrons of the ground state LS configuration.

Unlike LaCoO_3 the Co 3d t_{2g} states for spin-polarized $\text{La}_{0.5}\text{Ca}_{0.5}\text{CoO}_3$ are well separated from E_F , hence stabilizing the ferromagnetic state. This is evident from the DOS curve for $\text{La}_{0.5}\text{Ca}_{0.5}\text{CoO}_3$ shown in figure 4, where the ferromagnetic state with a magnetic moment of $1.2 \mu_B$ is obtained. One sees that the partial density of states for the Co t_{2g} orbitals in $\text{La}_{0.5}\text{Ca}_{0.5}\text{CoO}_3$ is very different from that in LaCoO_3 . The major peak near the top of the valence band in LaCoO_3 is now split into two subbands because of the exchange field, where one moves upwards towards the Fermi energy while the other moves deep below the Fermi energy. The partial density of states of Co e_g orbitals in $\text{La}_{0.5}\text{Ca}_{0.5}\text{CoO}_3$ is not so different from that of LaCoO_3 except for strong broadening. According to our ferromagnetic spin-polarized calculations, we assign a moment of $1.2 \mu_B$ to the IS state, which is in good agreement with experiment [16]. From our calculations the IS state turns out to be metallic. The reason for the metallic behaviour of the IS state is that the bands formed by e_g orbitals are broad and the band splitting is not strong enough to create a gap. DOS for this IS state shows that the nonbonding t_{2g} electrons are present at E_F mainly from spin-down state. Consequently, this state is energetically more stable than the LS state.

The electronic structure of $\text{La}_{0.5}\text{Ca}_{0.5}\text{CoO}_3$ shows that the doping-induced metallic state is very similar to that of the high-temperature metallic state of LaCoO_3 reported for example in [41]. Hence, the calculations on hole-doped LaCoO_3 are expected to give a better understanding about the nature of the temperature induced spin-state transition. It is suggested that the Ca doping favours the IS state by the introduction of $\text{Co}^{4+}(3d^5)$. The IS state of Co^{3+} possesses $S = 1$, namely a maximum magnetic moment of $M_{\text{Co}} = 2 \mu_B$. This corresponds to the purely ionic model; hybridization of Co 3d orbitals with the O 2p orbital and the band formation in the solid states can significantly renormalize this ionic value. Hence, the calculated magnetic moment of $1.2 \mu_B$ is smaller than the ionic value. One of the reasons for the stabilization of the IS state by hole doping is that the hole doping reduces the ionicity and enhances the covalent hybridization between Co and O.

The total DOS for LaCoO_3 in the LS state (figure 3(a)) shows that E_F is located in a deep valley, namely in a nonmagnetic state. The contribution of the density of states above the Fermi energy stems mainly from the t_{2g} electrons. Although the e_g bands are rather extended, their density of states at the Fermi energy is not negligible and they play a significant role in the metallic character of $\text{La}_{0.5}\text{Ca}_{0.5}\text{CoO}_3$.

The appearance of ferromagnetism upon hole doping in LaCoO_3 can be understood as follows: the reduction in valence electrons by the Ca substitution shifts E_F to the higher energy side of the valence band toward the peak position in DOS (figure 4). As a result, the Stoner criterion for band ferromagnetism becomes fulfilled and the metastable state is stabilized, which results in ferromagnetism. Moreover, if hybridization with the oxygen band is taken into account the stability of IS is accounted for.

In table 1 the occupation of different orbitals in both compounds is presented. In LaCoO_3 , having a low-spin (LS) ground state, the total e_g orbitals, which is formally empty, actually have an occupancy of about 1.05, resulting in 0.46 additional d electrons above the formal six-electron configuration. In the case of $\text{La}_{0.5}\text{Ca}_{0.5}\text{CoO}_3$, having an intermediate-spin (IS) ground state, we have a partially filled broad σ^* band, with the total number of e_g electrons increased by 0.47 as compared to the LaCoO_3 compound, and the number of t_{2g} electrons 0.78 less than in LaCoO_3 , yielding a practically unchanged total number of d electrons. Therefore, we used the notation σ^* in accordance with notation proposed in [12].

Some other points concerning the results obtained are worth mentioning. As one can see from figure 3, the occupied states closest to the Fermi energy in LaCoO_3 are mainly formed by oxygen states. However, in the $\text{La}_{0.5}\text{Ca}_{0.5}\text{CoO}_3$ case, which in our calculations is metallic (figure 4), the states near the Fermi level contain comparable weights of both Co e_g and O p orbitals.

4. Conclusion

In summary, we have performed full potential LAPW DFT calculations on $\text{La}_{1-x}\text{Ca}_x\text{CoO}_3$ ($x = 0, 0.5$). We have investigated the effect of Ca substitution on the electronic structure, and the interplay of electronic and magnetic properties of these compounds. Our results mean that the Ca substituting for La introduces hole states above the Fermi level with substantial Co 3d character and gives the metallic behaviour. The electronic structures predicted by spin-polarized DFT for both LaCoO_3 and $\text{La}_{0.5}\text{Ca}_{0.5}\text{CoO}_3$ are qualitatively correct. We can also mention that the calculated magnetic moment is found to be in good agreement with experiment.

Acknowledgments

We thank J-C Parlebas, C Demangeat and M-M Rohmer for helpful discussions. This work was supported by the Swiss National Science Foundation, the State Secretariat for Education and Science (COST Action D26) and the Paul Scherrer Institut.

References

- [1] Yan J-Q, Zhou J-S and Goodenough J B 2004 *Phys. Rev. B* **69** 134409
- [2] Zobel C, Kriener M, Bruns D, Baier J, Gruninger M, Lorenz T, Reutler P and Revcolevschi A 2002 *Phys. Rev. B* **66** 020402(R)
- [3] Raccah P M and Goodenough J B 1967 *Phys. Rev.* **155** 92
- [4] Señaris-Rodriguez M A and Goodenough J B 1995 *J. Solid State Chem.* **118** 323
Señaris-Rodriguez M A and Goodenough J B 1995 *J. Solid State Chem.* **116** 224
- [5] Asai K, Yoneda A, Yokokura O, Tranquada J M, Shirane G and Kohn K 1998 *J. Phys. Soc. Japan* **67** 290
- [6] Goodenough J B 1971 *Mater. Res. Bull.* **6** 967
- [7] Korotin M A, Ezhov S Yu, Solovjev I V, Anisimov V I, Khomskii D I and Sawatzky G A 1996 *Phys. Rev. B* **54** 5309
- [8] Yamagushi S, Okimoto Y and Tokura Y 1997 *Phys. Rev. B* **55** R8666
- [9] Radaelli P G and Cheong S-W 2002 *Phys. Rev. B* **66** 094408
- [10] Vogt T, Hriljac J A, Hyatt N C and Woodward P 2003 *Phys. Rev. B* **67** 140401
- [11] Maris G, Ren Y, Volotchaev V, Zobel C, Lorenz T and Palstra T T M 2003 *Phys. Rev. B* **67** 224423
- [12] Goodenough J B 1995 *J. Solid State Chem.* **116** 224
- [13] Kriener M, Zobel C, Reichl A, Baier J, Cwik M, Berggold K, Kierspel H, Zabara O, Freimuth A and Lorenz T 2004 *Phys. Rev. B* **69** 094417
- [14] Burely J C, Mitchell J F and Short S 2004 *Phys. Rev. B* **69** 054401
- [15] Baily S A and Salamon M B 2003 *J. Appl. Phys.* **93** 8316
- [16] Muta K, Kobayashi Y and Asai K 2002 *J. Phys. Soc. Japan* **71** 2784
- [17] Baily S A, Salamon M B, Kobayashi Y and Asai K 2002 *Appl. Phys. Lett.* **80** 3138
- [18] Ganguly R, Gopalakrishnan I K and Yakhmi J V 1999 *Physica B* **271** 116
- [19] Samoilov A V, Beach G, Fu C C, Yeh N-C and Vasquez R P 1998 *Phys. Rev. B* **57** R14032
- [20] Yeh N-C, Vasquez R P, Beam D A, Fu C-C, Huynh J and Beach G 1997 *J. Phys.: Condens. Matter* **9** 3713
- [21] Zock C, Haupt L, Todris B M, Asadov K, Zavatskii E A and Gron T 1995 *J. Magn. Magn. Mater.* **150** 253
- [22] Tolpygo S K, Mikhailov I G, Morozovsky A E, Yushchenko S K and Ryabchenko S M 1991 *Physica C* **185-189** 1097
- [23] Vasquez R P 1996 *Phys. Rev. B* **54** 14938
- [24] Tagushi H, Shimada M and Koizumi M 1982 *J. Solid State Chem.* **41** 329
- [25] Gai P L and Rao C N R 1975 *Mater. Res. Bull.* **10** 787
- [26] Patil S B, Keer H V and Chakrabarty D K 1979 *Phys. Status Solidi a* **52** 681
- [27] Bandyopadhyay A, Patil S B, Chakrabarty D K and Radhakrishnamurty C 1982 *Phys. Status Solidi a* **69** 441
- [28] Chakrabarty D K, Bandyopadhyay A, Patil S B and Shringi S N 1983 *Phys. Status Solidi a* **79** 213
- [29] Shannon R D 1976 *Acta Crystallogr. A* **32** 751
- [30] Ravindran P, Korzhavyi P A, Fjellvag H and Kjekshus A 1999 *Phys. Rev. B* **60** 16423

- [31] Blaha P, Schwarz K, Madsen G K H, Kvasnicka D and Luitz J 2001 *WIEN2k, An Augmented Plane Wave Plus Local Orbitals Program for Calculating Crystal Properties*, Vienna University of Technology, Austria (ISBN 3-9501031-1-2)
- [32] Blaha P, Schwarz K, Sorantin P and Trickey S B 1990 *Comput. Phys. Commun.* **59** 399
- [33] Singh D 1994 *Plane Waves, Pseudopotentials and the LAPW Method* (Dordrecht: Kluwer–Academic)
- [34] Madsen G H K, Blaha P, Schwarz K, Sjöstedt E and Nordström L 2001 *Phys. Rev. B* **64** 195134
- [35] Schwarz K, Blaha P and Madsen G K H 2002 *Comput. Phys. Commun.* **147** 71
- [36] Monkhorst H J and Pack J P 1976 *Phys. Rev. B* **13** 5188
- [37] Perdew J P and Zunger A 1981 *Phys. Rev. B* **23** 5048
- [38] Perdew J P, Burke K and Ernzerhof M 1996 *Phys. Rev. Lett.* **77** 3865
Perdew J P, Burke K and Wang Y 1996 *Phys. Rev. B* **54** 16533
- [39] Anisimov V I, Zaanen J and Andersen O K 1991 *Phys. Rev. B* **44** 943
- [40] Cococcini M and de Gironcoli S 2005 *Phys. Rev. B* **71** 035105
- [41] Ravindran P, Fjellvag H, Kjekshus A, Blaha P, Schwarz K and Luitz J 2002 *J. Appl. Phys.* **91** 291